



Natural Resources  
Canada

Ressources naturelles  
Canada

**GEOLOGICAL SURVEY OF CANADA  
OPEN FILE 7651**

**Chemostratigraphy of the late Pleistocene Dashwood Drift to  
Capilano Sediment succession using portable XRF  
spectrometry, Nanaimo, British Columbia, Canada**

**R.D. Knight, A.M.G. Reynen, E.C. Grunsky,  
H.A.J. Russell**

**2015**

**Canada** 



**GEOLOGICAL SURVEY OF CANADA  
OPEN FILE 7651**

**Chemostratigraphy of the late Pleistocene Dashwood Drift to  
Capilano Sediment succession using portable XRF  
spectrometry, Nanaimo, British Columbia, Canada**

**R.D. Knight, A.M.G. Reynen, E.C. Grunsky, H.A.J. Russell**

**2015**

© Her Majesty the Queen in Right of Canada, as represented by the Minister of Natural Resources Canada, 2015

doi:10.4095/295688

This publication is available for free download through GEOSCAN (<http://geoscan.nrcan.gc.ca/>).

**Recommended citation**

Knight, R.D., Reynen, A.M.G., Grunsky, E.C., and Russell, H.A.J., 2015. Chemostratigraphy of the late Pleistocene Dashwood Drift to Capilano Sediment succession using portable XRF spectrometry, Nanaimo, British Columbia, Canada; Geological Survey of Canada, Open File 7651, 1 .zip file. doi:10.4095/295688

Publications in this series have not been edited; they are released as submitted by the author.

## Table of Contents

1.0	Introduction .....	1
2.0	Surficial stratigraphy .....	1
	2.1 Dashwood Drift	
	2.2 Cowichan Head Formation	
	2.3 Quadra Sand	
	2.4 Vashon Drift	
	2.5 Capilnao Sediments	
	2.6 Salish Sediments – Postglacial	
3.0	Methods .....	4
	3.1 Reproducibility and precision of standards	
	3.2 Limits of detection	
	3.3 Erroneous analysis	
4.0	Results .....	12
	4.1 Chemostartigraphic trends – Cochrane borehole	
	4.1.1 Dashwood Drift	
	<i>Unit 1</i>	
	<i>Unit 2</i>	
	<i>Unit 3</i>	
	<i>Unit 4</i>	
	<i>Unit 5</i>	
	4.1.2 Cowichan Head Formation	
	4.1.3 Quadra Sand	
	4.1.4 Vashon Drift	
	4.1.5 Capilano Sediments	
	4.2 Chemostartigraphic trends – Spider borehole	
	4.2.1 Dashwood Drift	
	<i>Unit 1</i>	
	<i>Unit 2</i>	
	<i>Unit 3</i>	
	<i>Unit 4</i>	
	<i>Unit 5</i>	
	4.2.2 Cowichan Head Formation	
	4.2.3 Quadra Sand	
	4.2.4 Vashon Drift	
	4.2.5 Capilano Sediments	
5.0	Summary .....	26
6.0	Acknowledgements .....	28
7.0	References .....	28

## 1.0 Introduction

The Geological Survey of Canada in collaboration with the Regional District of Nanaimo has been completing a geological investigation in the Nanaimo Lowland region (Fig. 1) from Parksville to Bowser since 2009 in support a regional hydrogeology study. To better define the aquifer potential of the region a seismic reflection survey was completed and ground truthed with five boreholes (Fig. 1). Geochemical analyses by pXRF spectrometry were completed on the sediments collected from two of the five boreholes (GSC-BH-CHR and GSC-BH-SPI).

Results of these analyses are crucial to defining chemical and related mineralogical variations within sediments and augments sediment description, grain size data, downhole geophysical and stratigraphic correlations. Geochemical data also provides an opportunity for spatial correlation and establishment of a chemostratigraphic framework that complements other stratigraphic correlation techniques, for example lithostratigraphy and biostratigraphy. For groundwater studies the collection of geochemical data is often beyond the budget of most programs. However recent advances in portable X-ray fluorescence spectrometry (pXRF) as well as numerous studies on the comparison of these data with laboratory chemical analysis (Knight et al, 2013, Morris, 2009; Radu and Diamond, 2009, Stanley et al, 2009) indicate that this type of analyses is appropriate for the fine sand to clay-size fractions. This method has been successfully used to define the chemostratigraphy from a borehole in a Champlain Sea aquitard in southeastern Ontario (Knight et al., 2012) and for a borehole from the Spiritwood buried valley in southern Manitoba (Crow, et al., 2012 and Plourde et al., 2012). The integrated data sets provide fundamental information that can be used for defining chemical and mineralogical variations within aquifers and aquitards and are crucial to the development of basin stratigraphy, provenance and the production of accurate 3-dimensional basin models.

The primary objective of this Open File is to release data obtained from the use of a portable X-ray fluorescent spectrometer from a 130 m deep borehole (Cochrane) and a 117 m deep borehole (Spider) located near Nanaimo, B.C. (Fig. 1). Secondary objectives include analysis of the geochemical data within a stratigraphic context using principal component analysis and reference to individual elemental trends.

## 2.0 Surficial stratigraphy

The investigated well sites are located within the Georgia Basin (Gabrielse and Yorath, 1992), a structural depression that contains the Georgia Strait. An overview of the basins regional setting, structural history and late Cretaceous infill is presented in Mustard (1994). Quaternary fill in the Strait of Georgia has been extensively studied since Dawson (1878) reported shells in massive diamicton on Vancouver Island. The primary source of information on the surficial geology of the area is by Hicock (1980) and Hicock and Armstrong (1983) with recent work being carried out by Bednarski (2014) in the area from Deep Bay to Nanoose Bay. A number of authors have reviewed the glacial history of the area, (e.g. Fyles, 1963; Clague et al., 2005) and others (Hicock and Armstrong, 1981, 1983, 1985) have worked on aspects of the stratigraphy, chronostratigraphy, sedimentary facies, and process interpretations (Trettin, 2004; Clague et al., 2005 and references there in). Seven regional stratigraphic units are summarized here.

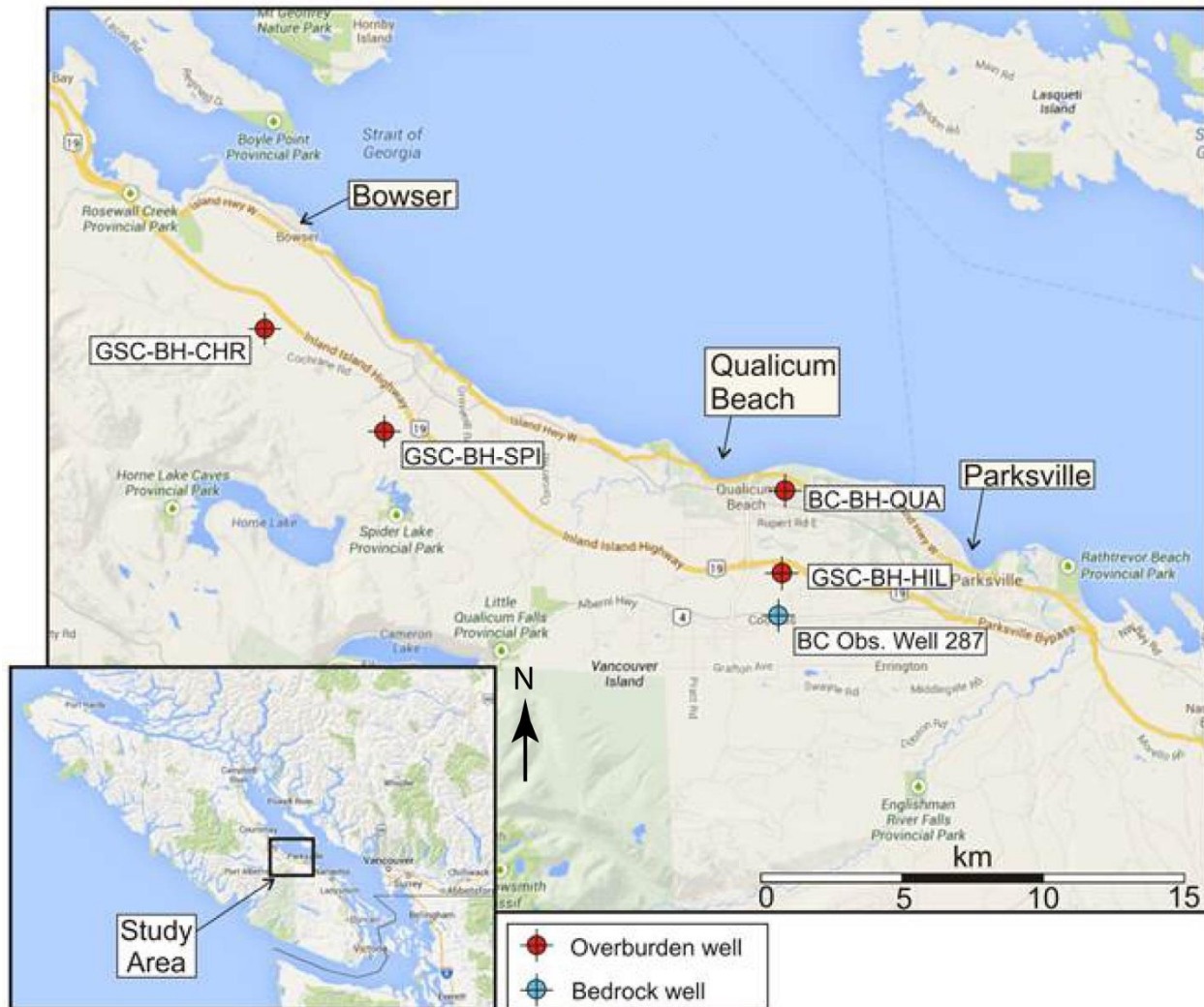


Figure 1. Location of the Nanaimo boreholes (from Crow et al., 2014).  
GSC-BH-CHR = Cochrane, GSC-BH-SPI = Spider.

## 2.1 Dashwood Drift

The oldest Quaternary deposits in the study area are exposed at the base of a few sea cliff sections. These sediments consist of unfossiliferous interbedded clay, silt, sand, and minor gravel. They were classified as the Maplegaurd Sediment by Fyles (1963) and later incorporated as the basal unit of the Dashwood Drift by Hicock and Armstrong (1983). Trettin (2004) identifies a number of facies changes regionally from previous work and highlights a lower and upper member of predominantly sand and diamicton, respectively. Fyles (1963) suggested a variety of depositional setting including, fine-grained river flood-plain deposits, lake sediments and glacial fluvial deposits. These lowermost sediments were not encountered in either the Cochrane or Spider boreholes.

The sediments of the Dashwood Drift that are encountered in the two boreholes consist of diamicton overlain by mud and gravel. The gravel is a mixture of plutonic lithologies derived from the Coast

Mountains and volcanic and sedimentary lithologies from the east coast of Vancouver Island. Depositional environments include a complex of glacial, glaciofluvial, ice-contact and glaciomarine to marine sediments (Hicock and Armstrong, 1983).

## **2.2 Cowichan Head Formation**

Cowichan Head Formation is up to 21 m thick and unconformably overlies the Dashwood Drift (Hicock and Armstrong, 1983). The formation has been divided into a lower member of clayey silt and sand with marine shells, and an upper member of sandy silt and gravel from volcanic and sedimentary rocks, commonly with reddish oxidized hues rich in fossil plant remains (Armstrong and Clague, 1977, Clague, 1976). The lower member is interpreted as glaciomarine whereas the upper member is attributed to estuarine and fluvial environments (Armstrong and Clague, 1977).

## **2.3 Quadra Sand**

The Quadra Sand may either sharply (erosionally - unconformably) or conformably overlie the Cowichan Head Formation and occurs over a broad area in the Georgia Depression, British Columbia and Puget Lowland, Washington (Clague 1976; Armstrong and Clague, 1977). It is up to 75 m thick and consists of horizontally and cross-stratified sand composed of quartz, feldspar, and lithic fragments of granitic provenance (Clague, 1976, 1977). The provenance and well sorted character imparts a ivory (white) colour to the unit. The sand is diachronous, becoming younger to the south away from its source in the Coast Mountains (Clague et al., 2005). The Quadra Sand is interpreted to be proglacial outwash deposited subaerially on floodplains and locally as deltaic deposits (Clague et al., 2005). This unit is a significant aquifer.

## **2.4 Vashon Drift**

Vashon Drift deposits are up to 60 m thick and unconformably overlie either Quadra Sand or older units. The Vashon Drift consists of sandy diamicton, with local mud rich, and sand and gravel facies (Fyles, 1963). Vashon Drift is interpreted as glacial till formed in a variety of ice-contact depositional (landform) settings including esker, deltas, and fans (Hicock and Armstrong, 1985).

## **2.5 Capilano Sediment**

Capilano Sediment unconformably overlies Vashon Drift and locally Quadra Sand. The sediment is up to 25 m thick (Bednarski unpublished) and consists of sand and gravel with minor diamicton. The sediment commonly fines upward. It is interpreted as a deglacial succession of coarse glaciofluvial outwash that becomes more distal upward.

## **2.6 Salish Sediments – Postglacial – Modern**

Salish Sediments are the youngest unit in the area, are generally < 5 m thick (commonly < 2 m) and consist of gravel, sand and mud (Fyles, 1963). Depositional processes are predominantly channel and floodplains along river valleys, deltaic sediments related to the modern sea, river and lake levels, and recent mass wasting (e.g. alluvial fans). These sediments were not encountered in either the Cochrane or Spider boreholes.



### 3.0 Methods

In 2011 the Geological Survey of Canada collected 17 seismic reflection profiles in the Nanaimo lowlands of British Columbia (Pugin et al., 2009). These profiles were used to locate targets for drilling three cored boreholes: Cochrane, Spider, and Hillier and one non-cored borehole: Qualicum. The boreholes are located between 40 and 60 km northwest of Nanaimo, B.C. (Fig. 1).

The boreholes were drilled in the winter of 2012-13 by Mud Bay Drilling (Borat Longyear) using a full-sized, truck-mounted Roto-Sonic drill (Fig. 2). Water with a biodegradable viscosity agent was used as drilling fluid. Onsite geological observations were carried out by GSC staff. Sediment core was collected from the Cochrane borehole starting at ground level. For the Spider borehole core was collected starting at 8 feet below ground level. Both holes were terminated before contact with bedrock. For each borehole, core was collected in 10 ft runs. The sediment cores were placed in a plastic sleeve, sealed with tape, boxed and shipped to GSC Ottawa for further logging and sampling. A suite of downhole geophysical logs, including magnetic susceptibility, apparent conductivity, P- and S- wave velocities, Gamma, and fluid temperatures were obtained for each borehole in March of 2013 (Crow et al. 2014).



Figure 2. Truck-mounted Roto-Sonic drill located at the Spider borehole.  
(photo by H.A.J. Russell).

Grain size was determined for each sample being analysed for geochemistry using a Camsizer particle scanner and a Lecotrac LT100 laser diffractometer. All grains > 2 mm in diameter were removed prior to this analysis. Numerical results are available in Appendix A and graphically displayed in Appendix A and B.

Prior to pXRF analyses the sediment was freeze-dried, disaggregated and sieved to  $<63\ \mu\text{m}$  (silt + clay) at the GSC Sedimentology Laboratories in Ottawa. The processed samples were placed in plastic vials and sealed with  $4\ \mu\text{m}$  thick SpectroCertified® mylar. Data were acquired using a handheld Thermo Scientific, Niton XL3t GOLDD XRF spectrometer equipped with Cygnit 50 kV, 2 watt Ag anode X-ray tube and a XL3 silicon drift detector (SDD) with 180,000 counts per second (cps) throughput, mounted to a test stand (Fig. 3). Samples were analyzed in Soil Mode which is recommended for elements expected to occur with  $< 1\%$  concentration. For the Spider borehole samples were also analyzed in Mining Mode, which is recommended for elements expected to occur with  $> 1\%$  concentration. Although these data are included in Appendix A they are not discussed. In order to honor the protocol used for previous borehole studies (Knight et al., 2012, Plourde et al., 2012) a dwell time of 60 seconds was used for each filter (Main, Low, and High), for a total of 180 seconds per analysis. However Knight et al., (2013) has found that dwell times as low as 30 seconds for some elements can return precise and accurate results.



Figure 3. Analysis of processed sediment samples using the pXRF spectrometer mounted in a test stand.

PXRF spectrometry was completed on 111 of the 115 sediment samples for the Cochrane borehole, four samples had an inadequate residue quantity for pXRF analyses. For the Spider borehole 119 samples were analysed (Appendix A and B).



The pXRF data are interpreted using single element trends from the base to the top of the boreholes. These distributions are then integrated using Principal Component Analysis (PCA) to reduce the number of variables and to explore multi-elemental associations within the data (Grunsky, 2010). The original geochemical data was transformed using a centered log ratio (CLR) to overcome the problem of closure. The PCA transformation uses linear combinations of elements and a measure of element association to identify geochemical variations over the depth of the drill core, giving a score for each sample for the given combination. Principal components are ordered from largest to smallest eigenvalue with each subsequent orthogonal component (eigenvector) displaying less variation in the data than the previous component (Fig. 4). The value of a point is defined as the score of the data as it is subsequently projected onto a new coordinate space representing both positive and negative relationships for each principal component. The weight or size of contribution of each element of the principal component calculation is defined as the loading. Comparing the score and loading plots identifies co-relationships between elements and positive and negative relationships of the elements. The relative change of these values and their trends display the behavior of the weighted grouping of elements (i.e. a change in the trend displays a change in the relationship of elements at that depth). Use of principal components can reveal relationships between elements that are co-related and most likely represent a variation in lithologic and provenance of the sediments (Grunsky, 2010). These scores can be scaled, fitted and plotted using a method described by Zhou et al., (1983) and implemented by Grunsky (2001). As the amount of variation for each principal component decreases the transformed data becomes noisy, which can be attributed to random error or under sampled processes. For this study scores for PC1 and PC2 are examined for the Cochrane borehole whereas PC1, 2, and 3 are examined for the Spider borehole. These principal component scores are plotted with respect to the stratigraphic section where it was observed that a cyclic variation occurred. Natural cubic splines (Hastie, 1992) were fitted to the scores as a function of stratigraphic depth.

Fifteen elements (As, Ba, Ca, Cr, Cu, Fe, K, Mn, Rb, S, Sr, Pb, Ti, V, Zn, and Zr) were detected in sufficient quantities to produce results using the pXRF spectrometer. The X-ray emission lines used to determine elemental concentrations in Soil Mode are listed in Table 1. Results are presented in Appendix A and displayed graphically in Appendix B.

### **3.1 Reproducibility and Precision of Standards**

Results of all analyses of standards are included with the sediment datasets in Appendix A. Two standards (Till-1 and Till-4) were analyzed after every 8 to 10 analyses of the borehole samples. A SiO<sub>2</sub> blank was analysed to determine the cleanliness of the pXRF window and sample stand environment. When data for the SiO<sub>2</sub> blank returned values for elements that should not be detected in greater amounts than trace the operating environment (test stand) was purged with compressed air and wiped clean with Isopropyl alcohol or Methanol until the operating environment was not contaminated. The SpectroCertified<sup>®</sup> Mylar polyester contains trace amounts of Ca and Fe. Some elements such as Ni, V, and Zr that are not listed as known impurities returned values above the detection limit on a few occasions and most likely represent internal detector noise. A study into the precision, accuracy, instrument drift, dwell time optimization and calibration of pXRF spectrometry for reference materials including Till-1 and Till-4 is available from Knight et al., (2013).

Summary statistics for Till-1 and Till-4 determined during analyses of samples from both boreholes are presented in Tables 2 to 5. For each element detected in a given standard, the count, minimum value, maximum value, mean, standard deviation, relative standard deviation (%RSD), and %error are listed. The %error column contains the difference between the mean and recommended value. Low absolute values in this column indicate that the element is measured accurately; high absolute values indicate that a calibration curve is required to correct the data or that the data is not reliable. As an example Ni values obtained from Till-1 during analyses of the Cochrane samples (Table 2) has a %error of 246. Values returned by the pXRF were often greater than 3 times the recommended value. Thus chemostratigraphy for Ni was not plotted.

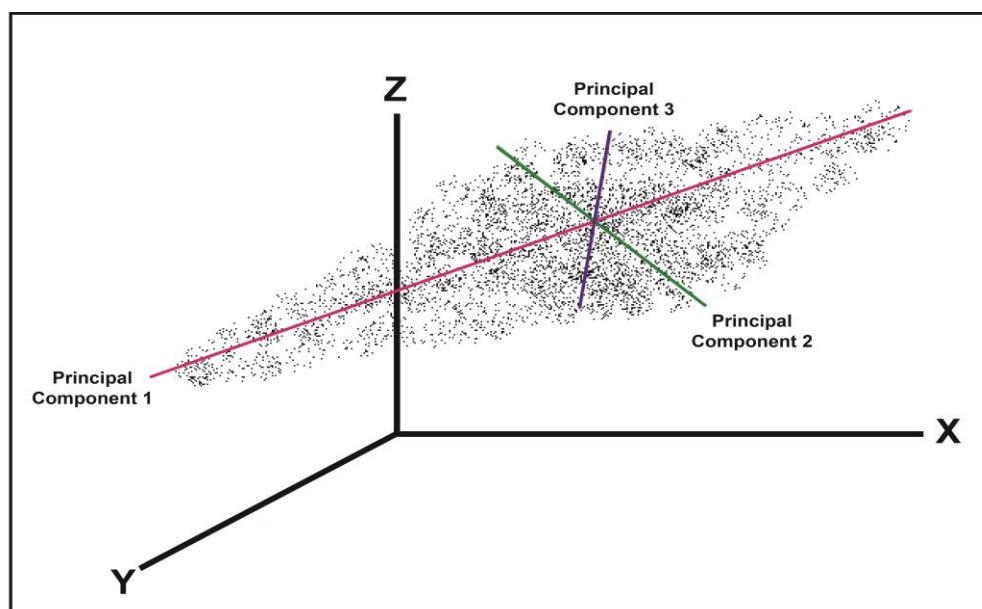


Figure 4. A hypothetical data set projected in 3-dimensions displaying the relationships between the 3 main principal components. From Whitbread, (2004) after Rock, (1988).

Similarly V values from Till-4 obtained during the collection of Spider data has a %error of 85, a mean value of 124 ppm compared to a recommended value of 67 ppm. However it is useful to plot V since chemostratigraphy utilizes the relative changes in concentration, making high precisions more important than accuracy. It is important to note that the precision and accuracy are affected by concentration. Lower concentrations tend to result in lower precision, and thus higher %RSD.

Element	Line	Energy (keV)	Window Low (keV)	Window High (keV)	Filter
As	K $\alpha_1$	10.54	10.33	10.73	Main
Ba	K $\alpha_1$	32.19	31.70	32.70	High
Ca	K $\alpha_1$	3.69	3.50	3.89	Low
Cd	K $\alpha_1$	23.17	22.60	23.60	High
Co	K $\alpha_1$	6.93	6.73	7.13	Main
Cr	K $\alpha_1$	5.41	5.24	5.59	Low
Cs	K $\alpha_1$	30.97	29.50	31.50	High
Cu	K $\alpha_1$	8.05	7.84	8.24	Main
Fe	K $\alpha_1$	6.40	6.20	6.60	Main
Hg	L $\alpha_1$	9.99	9.79	10.18	Main
K	K $\alpha_1$	3.31	3.10	3.49	Low
Mn	K $\alpha_1$	5.90	5.70	6.10	Main
Mo	K $\alpha_1$	17.48	17.23	17.68	Main
Ni	K $\alpha_1$	7.48	7.35	7.67	Main
Pb	L $\beta_1$	12.61	12.40	12.80	Main
Rb	K $\alpha_1$	13.39	13.18	13.60	Main
S	K $\alpha_1$	2.31	2.20	2.45	Low
Sb	K $\alpha_1$	26.36	25.90	26.90	High
Sc	K $\alpha_1$	4.09	3.90	4.19	Low
Se	K $\alpha_1$	11.22	11.01	11.41	Main
Sn	K $\alpha_1$	25.27	24.70	25.70	High
Sr	K $\alpha_1$	14.16	13.95	14.38	Main
Te	K $\alpha_1$	27.47	27.00	28.00	High
Th	L $\alpha_1$	12.97	12.80	13.15	Main
Ti	K $\alpha_1$	4.51	4.21	4.70	Low
U	L $\alpha_1$	13.61	13.48	13.90	Main
V	K $\alpha_1$	4.95	4.80	5.10	Low
W	L $\alpha_1$	8.40	8.26	8.49	Main
Zn	K $\alpha_1$	8.64	8.49	8.83	Main
Zr	K $\alpha_1$	15.77	15.53	15.98	Main

Table 1: X-ray energy intensities used to determine elemental concentrations in Soil Mode, as provided by Niton.

### 3.2 Limit of Detection

For this study the limit of detection (LOD) using pXRF spectrometry is defined as 2 standard deviations of the individual measurements taken throughout the 180 second analysis. It should be noted that for some sediments (e.g. Quadra Sand) two elements (As and S) returned analyses lower than the LOD. When this occurred, the point was plotted on the chemostratigraphy graphs using the LOD value. Elements detected by each filter and the corresponding lower limits of detection are listed in Table 6.

### 3.3 Erroneous Analysis

During analyses of the Cochrane borehole samples three results obtained for Till-1 returned either very low or very high concentrations for the majority of elements and are considered to be erroneous. The results were removed from the dataset presented in Appendix A. This emphasizes the importance of monitoring results in real time to ensure that operating conditions are optimal. No unexplained or erroneous data was collected from the borehole samples.

	Recommended Value (ppm)	Count	Mean (ppm)	%error	Std Dev (ppm)	%RSD	Minimum (ppm)	Maximum (ppm)
<b>As</b>	18	22	18	0	1.2	6.61	16	20
<b>Ba</b>	702	22	860	22.5	18	2.05	817	887
<b>Ca</b>	19440	22	17536	-9.8	163	0.93	17237	17862
<b>Co</b>	18	14	158	777.8	27	17.11	121	226
<b>Cr</b>	65	22	34	-47.7	5	13.31	24	41
<b>Cs</b>	<i>1</i>	22	<i>46</i>	<i>4502</i>	<i>2.41</i>	<i>5.24</i>	<i>42</i>	<i>51</i>
<b>Cu</b>	47	22	61	29.8	5	8.77	53	71
<b>Fe</b>	48100	22	40820	-15.1	256	0.63	40383	41287
<b>K</b>	18429	22	15797	-14.3	2	1.38	15427	16290
<b>Mn</b>	1420	22	1367	-3.7	35	2.54	1284	1420
<b>Mo</b>	2	22	5	150	1.5	33.2	1.5	8.2
<b>Ni</b>	24	22	83	246	7.4	8.95	70	97
<b>Pb</b>	22	22	13	-40.9	1.66	12.89	10	16
<b>Rb</b>	44	22	41	-6.8	0.9	2.28	39	43
<b>S</b>	< 500	22	185	-63	90	48.55	138	380
<b>Sr</b>	291	22	268	-7.9	3	1.12	262	274
<b>Th</b>	5.6	21	4.27	-23.7	0.92	21.61	2.83	6.67
<b>Ti</b>	5990	22	5441	-9.2	95	1.75	5272	5579
<b>U</b>	2.2	4	5.35	143	0.72	13.40	4.87	6.42
<b>V</b>	99	22	155	56.6	10	6.41	122	169
<b>Zn</b>	98	22	91	-7.1	2.8	3.02	86	95
<b>Zr</b>	502	22	574	14.3	6.0	1.04	560	585

Table 2. Summary statistics of Till-1 by pXRF spectrometry for the Cochrane borehole. Italics represent data obtained from reference materials that were less than the limits of detection for borehole samples.

	Recommended Value (ppm)	Count	Mean (ppm)	%error	Std Dev (ppm)	%RSD	Minimum (ppm)	Maximum (ppm)
As	18	17	18	0	1.2	6.93	16	21
Ba	702	17	867	23.5	18.5	2.14	835	896
Ca	19440	17	17470	-10.1	254	1	169327	17808
Co	18	3	169	838.9	65.6	38.82	128	245
Cr	65	17	44	-32.3	4.74	10.75	35	51
Cs	1	17	47	4600	3.02	6.40	40	52
Cu	47	17	59	25.5	4.87	8.25	51	67
Fe	48100	17	40934	-14.9	253	1	40369	41272
K	18429	17	15749	-14.5	157	1	15433	15957
Mn	1420	17	1368	-3.7	29	2.1	1317	1415
Mo	2	3	5	150	1.93	38.2	3.1	7
Ni	24	17	84	250	8.1	9.58	61	98
Pb	22	17	12	-45.5	1.69	13.97	8	15
Rb	44	17	41	-6.8	0.63	1.55	40	42
S	< 500	7	406	-18.8	75	18.48	329	516
Sr	291	17	270	-7.2	1.75	0.65	267	272
Th	5.6	17	4.19	-25.5	1.11	26.57	2.7	5.9
Ti	5990	17	5459	-8.9	113	2	5137	5611
U	2.2	10	5.62	155.5	0.99	17.57	4.58	7.8
V	99	10	165	66.7	14	8	132	187
Zn	98	17	92	-6.1	3.35	3.65	84	97
Zr	502	17	569	13.3	7.72	1.36	556	581

Table 3. Summary statistics of Till-1 by pXRF spectrometry for the Spider borehole. Italics represent data obtained from reference materials that were less than the limits of detection for borehole samples.

	Recommended Value (ppm)	Count	Mean (ppm)	%error	Std Dev (ppm)	%RSD	Minimum (ppm)	Maximum (ppm)
As	111	19	102	-8.1	2.6	2.58	98	108
Ba	395	19	454	14.9	18.7	4.11	421	486
Ca	8934	19	7824	-12.4	123	1.57	7651	8032
Co	395	10	146	-63	23.8	16.28	108	185
Cr	53	19	26	-50.9	4.3	16.57	18	34
Cs	12	19	25	108	3.4	13.75	18	32
Cu	237	19	215	-9.3	5.77	2.65	206	225
Fe	39700	19	33039	-16.85	222	0.67	32597	33504
K	26980	19	23709	-12.1	377	1.59	23192	24449
Mn	490	19	442	-9.8	19.3	4.37	405	473
Mo	16	19	20	25	1.5	7.78	17	22
Ni	17	19	55	224	9.1	16.62	44	79
Pb	50	19	43	-14	2.47	5.74	39	47
Rb	161	19	152	-5.6	1.7	1.12	148	155
S	800	19	576	-28	104	18.03	320	762
Sr	109	19	105	-3.7	1.23	1.13	103	108
Th	17.4	19	42	141	1.5	3.61	39	45
Ti	4840	19	5951	23	79	1.32	5712	6127
U	5	9	8.15	63	1.5	18.63	6.11	10.52
V	67	19	117	74.6	8.6	7.32	101	137
W	204	19	186	-8.8	11.9	6.40	164	203
Zn	70	19	65	-7.1	2.9	4.46	61	71
Zr	385	19	437	13.5	12.1	2.77	419	454

Table 4. Summary statistics of Till-4 by pXRF spectrometry for the Cochrane borehole. Italics represent data obtained from reference materials that were less than the limits of detection for borehole samples.



	Recommended Value (ppm)	Count	Mean (ppm)	%error	Std Dev (ppm)	%RSD	Minimum (ppm)	Maximum (ppm)
As	111	17	104	-6.3	2.11	2.03	100	108
Ba	395	17	452	14.4	10.6	2.34	429	471
Ca	8934	17	7849	-12.1	87	1.1	7647	7989
Co	395	3	146	-63	23.8	16.28	108	185
Cr	53	17	32	-39.6	5.14	16.06	17	41
Cs	12	17	23	91.7	2.46	10.52	20	27
Cu	237	17	217	-8.4	5.41	2.50	208	230
Fe	39700	17	33239	-16.3	203	0.6	32916	33656
K	26980	17	23811	-11.7	214	0.9	23521	24406
Mn	490	17	443	-9.6	25	5.6	399	498
Mo	16	17	17.9	11.9	1.38	7.70	15	20
Ni	17	17	57	235	7.42	13.12	46	71
Pb	50	17	41	-18	1.31	3.20	39	43
Rb	161	17	152	-5.6	1.64	1.08	148	154
S	800	17	624	-22	95	15.16	422	802
Sr	109	17	106	-2.8	1.01	0.95	104	107
Th	17.4	17	42.7	145	1.25	2.94	40.7	45.2
Ti	4840	17	4612	-4.7	56	1.2	4530	4725
U	5	16	13	160	2.91	22.72	6	18
V	67	17	124	85	9.6	7.76	106	146
W	204	17	179	-12.3	8.66	4.83	162	194
Zn	70	17	65	-7.1	3.10	4.76	61	70
Zr	385	17	426	10.6	12.3	2.89	409	467

Table 5. Summary statistics of Till-4 by pXRF spectrometry for the Spider borehole. Italics represent data obtained from reference materials that were less than the limits of detection for borehole samples.

Element	Matrix		Filter
	SiO <sub>2</sub>	SiO <sub>2</sub> + Fe +Ca	
As	4	7	High
Ba	35	45	Low
Ca	40	N/A	Low
Cu	10	13	Low
Cr	10	22	Main
Fe	25	N/A	Main
K	45	150	Low
Mn	35	50	Main
Mo	3	3	Main
Ni	25	30	Main
Rb	3	3	Main
S	75	275	Low
Sc	10	75	Main
Sr	3	3	Low
Ti	20	60	Low
V	10	25	Low
Zn	7	10	Main
Zr	3	4	Main

Table 6. Elements detected in the Nanaimo and Spider boreholes with corresponding detection limits for the pXRF using two matrix configurations and the filters used to detect these elements, Thermo Scientific

## 4.0 Results

In glaciated terrains of the late Pleistocene the <0.063mm size fraction of unconsolidated sediment represents crushed bedrock detritus, mineral grains, and grain fragments that are often un-weathered (McMartin and McClenaghan, 2001). For sediments analysed in the two boreholes Na and K likely represent granitic provenance, Ca represents carbonate terrains, while Fe, Co, Cr, Ni, V, and Zn represent volcanic source rocks. Until mineralogy (X-ray diffraction) of the sediments is undertaken pXRF spectrometry can only infer generalizations with regards to source rock types.

The relationship of grain size to the interpretation of the pXRF derived geochemistry has been discussed in Zhu et al., (2011) and Knight et al., (2012). Downhole grain size data are presented in Appendix A and plotted with pXRF derived concentrations in Appendix B. For both boreholes the Dashwood Drift has a greater abundance of silt and clay compared to the overlying sediments. The Quadra Sands display lower abundance of silt and clay with commensurate greater abundance of sand compared to the underlying and overlying sediments. The Vashon Drift displays an increase in clay compared to both the underlying Quadra Sand and the overlying Capilano Sediments. Sand content of the Capilano Sediments is greater than the underlying Vashon Drift.

### 4.1 Chemostratigraphic Trends – Cochrane borehole

Basal sediments of the Cochrane borehole are assigned to the Dashwood Drift and consist of 2 diamicton horizons separated by a mud/clay horizon. These sediments are overlain by a coarsening upwards sequence (mud to medium grained sand) through the Cowichan Head Formation to the overlying Quadra Sand. The lower half of the Quadra Sand consists of medium grained sand while the upper half consists primarily of fine grained sand with coarse grained sand horizons. The top 10 meters of the Quadra Sand consist of medium grained sand with pebbles. These sediments are overlain by the Vashon Drift, a sandy diamicton. Uppermost sediments consist of a lower mud/clay unit overlain by fine-grained sand with organic matter assigned to the Capilano Sediments.

Chemostratigraphy of the Cochrane borehole is discussed with respect to changes in the trend of concentration of single element chemistry (Appendix B) as well as multi-element principal component analyses. Individual elemental concentrations are plotted with depth adjacent to the stratigraphic section for the Cochrane borehole and displayed in Appendix B. Figure 5 displays the centered log ratio transformed geochemical data for principal components (PC) 1 and 2 plotted adjacent to the Cochrane borehole stratigraphic section.

Elements of similar relationship are plotted on Figure 6 as a positive correlation and elements with an opposite relationship display a negative correlation. The inset plot on Figure 6 displays the variation of the lengths of axes of each principal component. In this inset diagram little variation in the data occurs from PC3 onwards, thus only PC1 and PC2 are considered to be significant.

PC1 is dominated by a positive co-relationship for Ba, Ca, K, Mo, Sr and Zr with high scores being given to Ca and Sr (Fig. 6) and negative scores for As, Cu, Cr, Fe, Mn, Ni, Ti, V, and Zn (Fig. 6).

PC2 is dominated by a positive co-relationship of scores for Ca, Fe, Mo, Sr, Ti, V, and Zr with high scores for Fe (Fig. 6) and a negative relationship for As, Ba, K, S, Ni, Rb, and Zn (Fig. 6).

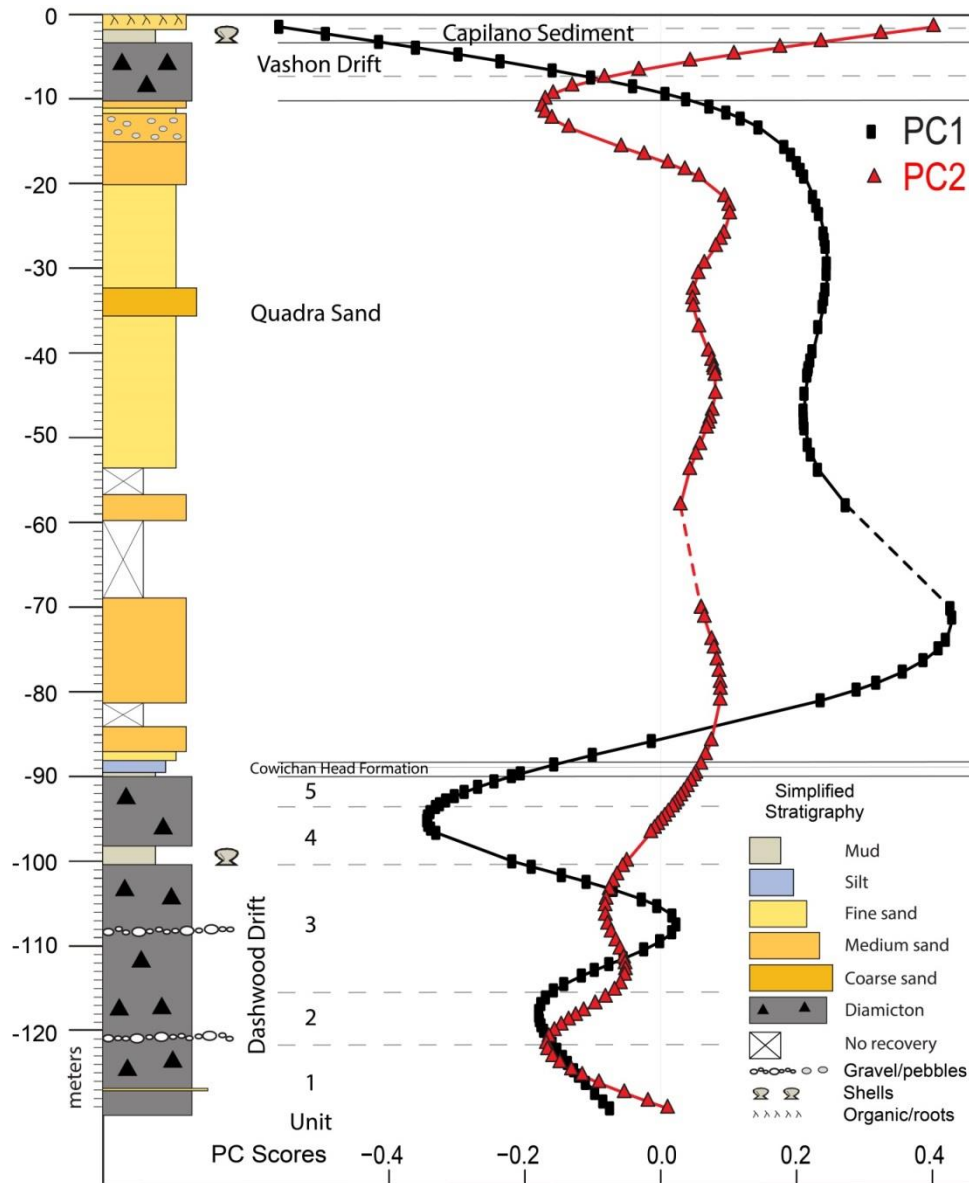


Figure 5. Centered log ratio transformed geochemical data for PC1 and PC2 plotted adjacent to the Cochrane borehole stratigraphic section.

#### 4.1.1 Dashwood Drift

For the basal Dashwood Drift there were 49 analyses determined from the Cochrane borehole. These sediments can be subdivided into five units based on changes in the trend single elemental concentrations, principal component analyses results of multiple related elements and/or changes in grain size. The units may not correspond to visual changes in sediments (eg. Unit 4/5 boundary) but do represent a shift in provenance and/or depositional processes. For most elements their concentrations are proportional to changes in abundance of silt and/or clay. However there are sediment horizons where a change in a single elemental concentration is not reflected by a change in grain size. For example, there is a sharp decrease in abundance of Ca and Sr and an increase in abundance for K, Mn,

Rb, and Zn at a depth of 115.5-121.5 meters (Fig. 7) where there is little to no change in grain size from the unit below or above. Some of these unit subdivisions are further substantiated by downhole magnetic susceptibility and apparent conductivity (Crow et al, 2014). For the Cochrane borehole the contact between the Dashwood Drift and the overlying Cowichan Head Formation brown muds consists of a sharp boundary.

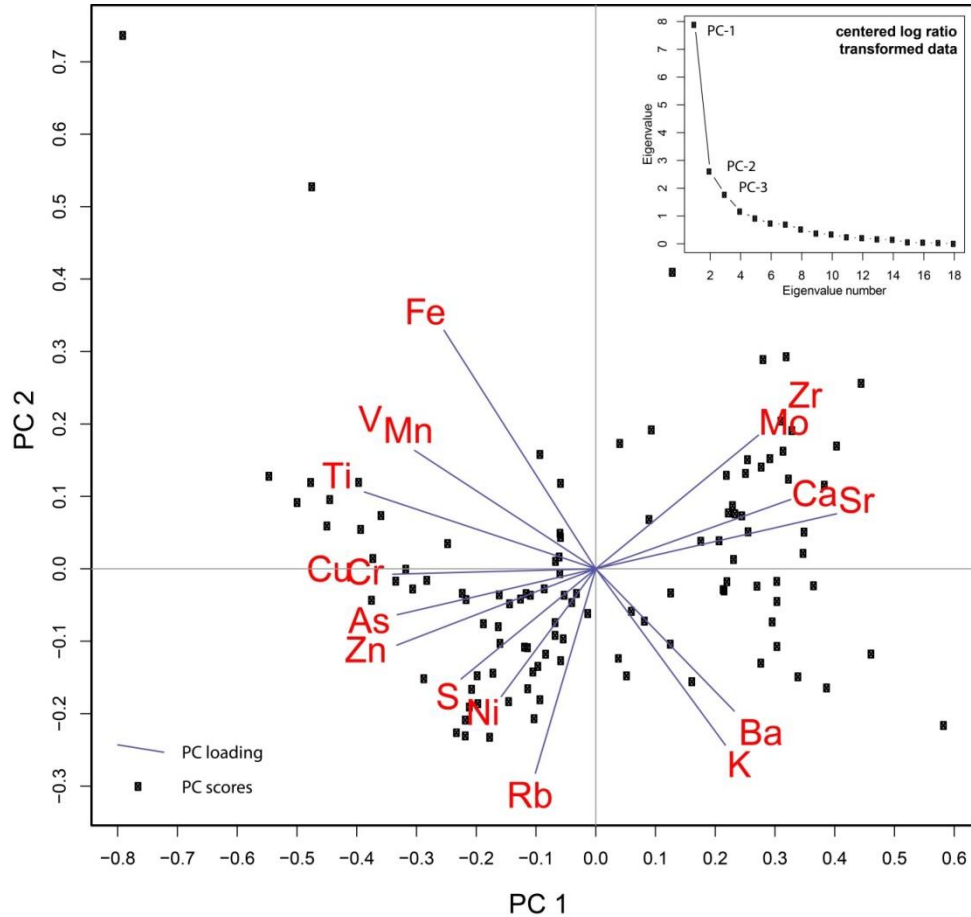


Figure 6. Principal component loading and scores for PC1 and PC2 for the Cochrane borehole data. Elements of similar relationship are plotted as a positive correlation while elements with an opposite relationship plot as a negative correlation. The inset diagram displays the eigenvalues and the number of eigenvectors.

### Unit 1

Nine analyses were determined from the approximately 7 + metres thick unit. A thin horizon of sand at a depth of 127 meters (Fig. 7) is reflected by an increase in concentration of Ca, Cr, Fe, V, and Zr, with a corresponding decrease in both K and Rb. It should be noted that the concentration of Sr does not seem to be affected by this sand horizon (Appendix B). Unit 1 is differentiated from overlying Unit 2 by changes in the trends of Ca, Cu, K, Mn, Rb and Zn.

### Unit 2

The contact between the underlying Unit 1 and Unit 2 occurs at the base of a gravel / pebble horizon. This unit is 7 meters thick, and displays a minor decrease in sand content with an increase in silt compared to unit 1. Analyses were determined for 9 samples. Results display a marked decrease in Ca from a mean of 33520 ppm for unit 1 to mean of 27255 ppm for unit 2, and a slight decrease in Sr from a mean of 238 ppm compared to a mean of 298 ppm for Unit 1 (See Appendix A). The transition from Unit 1 to Unit 2 is reflected in a change from a negative to more positive co-relationship of PC2 (Fig.5). Single element concentrations for K, Rb, (Fig. 7) Mn, and Zn all have higher values in Unit 2 compared to the underlying Unit 1. However some elements such as Fe, Ti, V, and Zr display little to no change between the units (Appendix B).

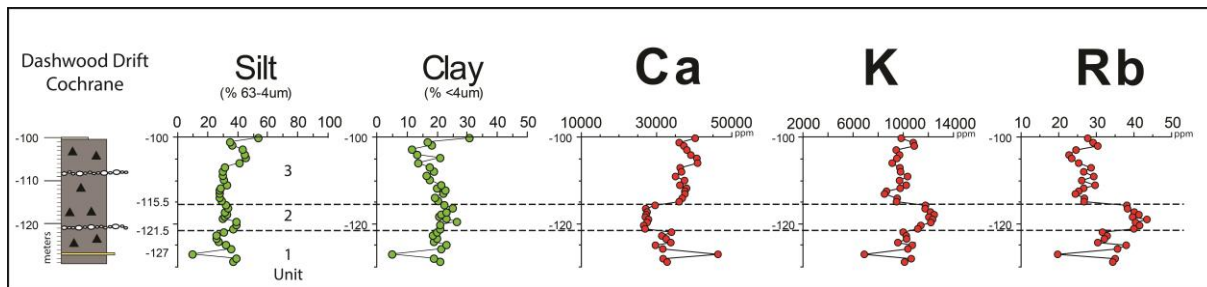


Figure 7. At a depth from 115.5 and 121.5 meters there is a decrease in Ca concentrations and an increase in K and Rb concentrations without any significant change in silt or clay content. At a depth of 127 meters a decrease in silt and clay (sand horizon) is marked by a significant change in several elements including Ca, K, and Rb.

### Unit 3

Sixteen analyses were determined from this 15 m thick unit. The unit displays a slight coarsening upwards trend from a decrease in clay and a corresponding increase in silt (Fig. 7). The inflection points of the trend curves for both PC1 and PC2 (Fig. 5) do not correspond to the exact depth of the change from unit 2 to unit 3, as defined by the increase in concentration of Ca (Fig. 7), but do display a shift for PC1 just below the contact and for PC2 just above the contact. There is a small increase in silt and sand in the upper 3-5 m of unit 3 (101-106 meters in depth, that is reflected in a decrease in concentration of Cr, Cu, Fe, Ti, V, and Zn (Fig. 8) and a minor increase in the concentration of Ba, Ca, K, Sr and Zr. Across the lower 3 units Sr, Ti, and V display little change until the top of unit 3 where Sr decreases and Ti and V increase in concentrations. PC 1 however shows a marked change from positive scores to negative scores corresponding to the gravel horizon observed at a depth of 108 meters (Fig. 5).

### Unit 4

The contact between Unit 3 and the overlying Unit 4 occurs between the top of the diamicton and the overlying clay (Fig. 8). Eight analyses were determined from this 11.5 meter thick unit. The lower and upper contact of this unit is defined by the concentration of S. The upper contact occurs within the upper diamicton of the Dashwood Drift. Compared to unit 3, unit 4 displays a marked decrease in sand and a corresponding increase in both silt and clay. At the contact between unit 4 and 5 there is a further drop in sand content. This unit contains S concentrations with a mean of 1053 ppm compared to a range of mean values from 486- 248 ppm for the other units (Appendix A). Unit 4



deviates from the units below by increases in the concentration of As, Ca, Cr, Cu, Fe, Mn, S, Ti, V, and Zn. There are also decreases in the concentration of Ba, K, Rb, Sr and to minor degree Zr. The change from unit 3 to 4 is reflected in a shift from positive to negative scores for PC1.

### Unit 5

Seven analyses were determined within this 4 meter thick unit. The unit is characterized by an upwards decreasing concentration of Ca from 264 ppm at the base to 187 ppm at the top of the unit. S concentrations decrease to below detection limits. Both units 4 and 5 display an upward increase in the concentration of Cr, Cu, Ti, and V, and a decrease in concentration of K and Sr (Appendix B). Zr concentrations remain the same throughout both units 4 and 5. The upper contact of unit 5 corresponds to a shift in trend from negative to more positive PC1 scores.

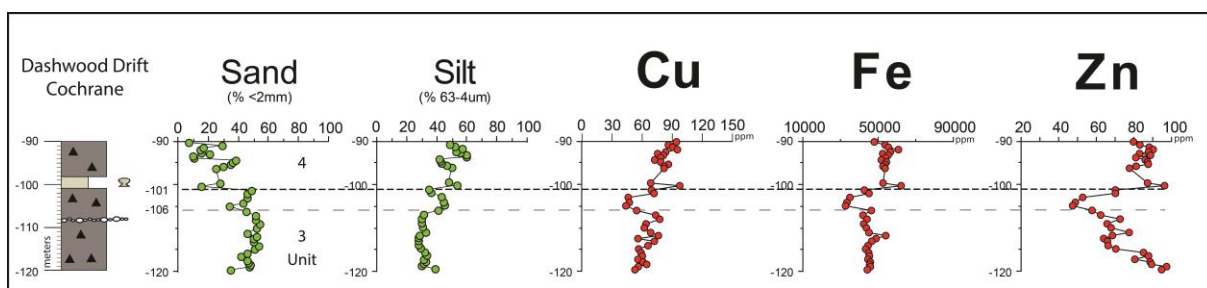


Figure 8. At a depth between 101 and 106 meters there is an increase in the sand and silt content and a corresponding decrease in Cu, Fe, and Zn concentrations.

### 4.1.2 Cowichan Head Formation

The Cowichan Head Formation is 2 meters thick. Two samples were collected for pXRF spectrometry. For most elements in the Cochrane borehole the concentration of these samples represents a transition from the underlying Dashwood Drift and the overlying Quadra Sand (Appendix B). The lower sample often is similar in elemental concentrations to that of the underlying Dashwood Drift unit 5 values and the upper sample is similar in elemental concentrations to the overlying Quadra Sand (eg: Cr, Cu, Fe and V). This is also displayed in the large shift from negative PC1 scores in the underlying Dashwood Drift unit 5 to positive PC1 scores in the overlying Quadra Sand (Fig. 5). Previous work by Alley (1979) indicates a lag deposit in some localities between the Dashood Drift and the Cowichan Head Formation. This lag deposit was not observed in either the Cochrane or Spider boreholes.

### 4.1.3 Quadra Sand

For the 78 m thick Quadra Sand 48 analyses were analysed. The sand displays a marked decrease in elemental abundances compared to both the underlying and overlying sediments for As, Cu, Fe, (S), Ti, V, and Zn whereas there is a marked increase in elemental abundances for Ca and Sr (Fig. 9). These trends in elemental concentrations correlate with a decrease in silt and clay and an increase in sand (Fig. 9). For Sr the mean of the concentration for the Dashwood Drift is 285 ppm, for the Cowichan Head Formation, 201 ppm and for the Vashon Drift 262 ppm, compared to the Quadra Sand with a mean concentration of 511 ppm. PC1 displays a strong shift to positive scores in the lower portion of the Quadra Sand followed by a slight shift towards negative scores in the mid portion of the sands (Fig. 5). This is followed by a further slight shift towards more positive scores at a depth of 40 meters before a

shift to strong negative scores to the top of the borehole. PC 2 displays several shifts (~5) in the trend of scores throughout the sands with a strong inflection at the contact with the overlying sandy Vashon Drift (Fig. 5).

#### 4.1.4 Vashon Drift

For the 7 m thick Vashon Drift 8 analyses were determined. Vashon Drift can be differentiated into an upper and lower unit based on variations in elemental abundances and changes in both the silt and clay content. Ca (Fig. 10), Cu, and Sr (Fig. 9) display a much lower concentration in the basal 4 samples and sharp increase in concentration for the upper 4 samples. Furthermore, Rb (Fig. 10), As, K, and Zn (Appendix B) display the opposite trend with higher concentrations in the lower four samples compared to the upper four. Elements such as Fe (Fig. 10), Ba, Mn, and especially Ti, and V and to a lesser degree Zr display no change with depth (Appendix B). For both the Vashon Drift and Capilano Sediments PC1 continues the trend towards negative scores that was established in the upper 10 meters of the Quadra Sand (Fig. 5). PC 2 displays a sharp inflection in a trend to negative scores to a trend towards positive scores at the contact between the Quadra Sand and the Vashon Drift. This trend continues to the top of the borehole (Fig. 5).

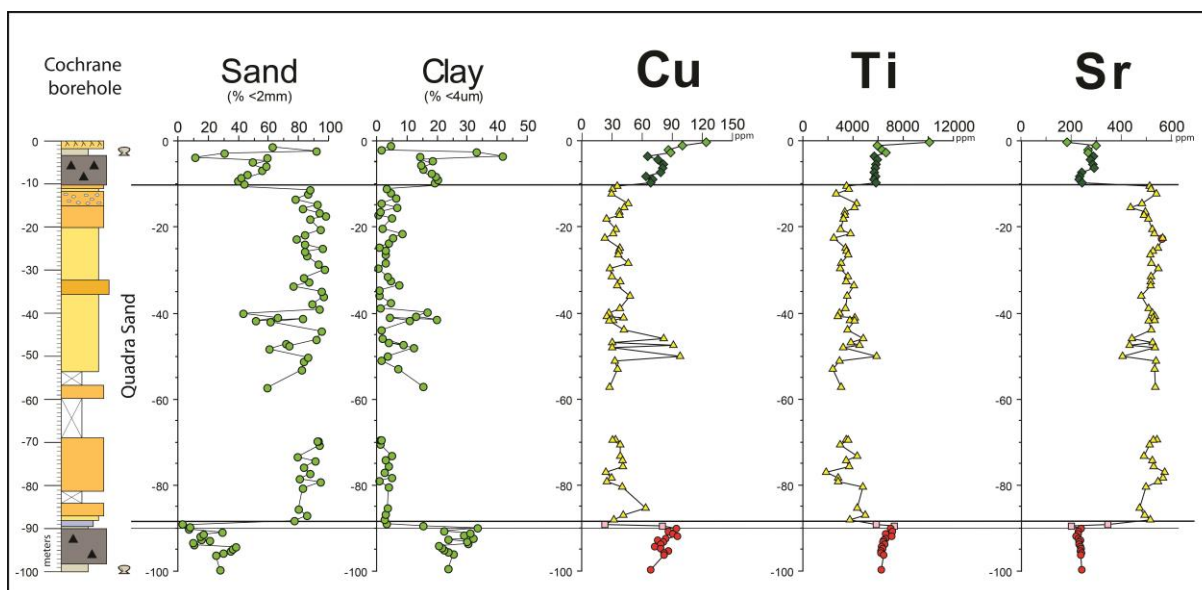


Figure 9. Quadra Sand is recognized by an increase in sand content and a decrease in clay content. Geochemically several elements including Cu and Ti display a decrease while Sr displays an increase in concentration's from both the underlying and overlying sediments.

#### 4.1.5 Capilano Sediments

For the 3 m thick Capilano Sediments 4 analyses were determined. With such a low number of samples it is difficult to ascertain geochemical trends with any degree of certainty however there is a decrease in concentration from the base of the Capilano Sediments upwards for Ba, Ca, K, Rb, and Zn. Similarly there is an increase in the concentration for Cu, Fe, Mn, and V (Fig. 10). The grain size for this interval decreases in clay and silt with a corresponding increase in sand however there is no direct relationship between the trends in concentration and the variations in grain size.

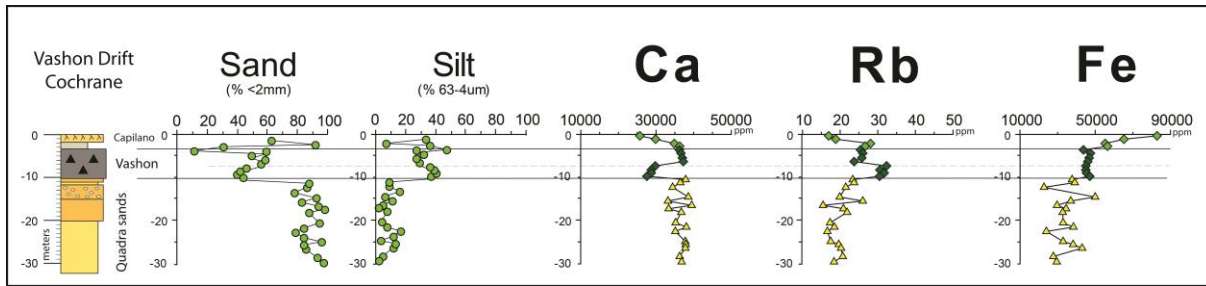


Figure 10. Vashon Drift is divided into 2 units, differentiated by minor changes in sand and silt content and distinctive change in some element concentrations such as Ca and Rb. Note that some elements such as Fe display little variation between the upper and lower portion of the Vashon Drift.

## 4.2 Chemostratigraphic Trends – Spider borehole

Basal sediments of the Spider borehole are assigned to the Dashwood Drift and consist of 3 diamicton horizons separated by a mud/clay horizon. These sediments are overlain by a coarsening upwards sequence (mud to coarse grained sand) similar to the Cochrane borehole. At Spider these sediments are overlain by a second coarsening upwards sequence from fine sand to coarse sand and gravel. In turn these sediments are overlain by a fining upwards sequence to a several meter thick silt horizon. These coarsening and fining upwards sequences are assigned to the Cowichan Head Formation. A sharp increase in sand content marks the contact with the overlying Quadra Sand. Opposite to the Cochrane borehole the lower half of the Quadra Sand consists predominantly of fine grained sand while the upper half consists primarily of fine and medium grained sand. These sediments are overlain by the Vashon Drift, a sandy diamicton that is thinner in comparison to the Cochrane borehole. Uppermost sediments consist of fine-grained sand assigned to the Capilano Sediments.

Individual elemental concentrations and grain size data are plotted with depth adjacent to the stratigraphic section for the Spider borehole and displayed in Appendix B. Centered log ratio transformed geochemical data for principal components (PC) 1, 2 and 3 are plotted adjacent to the stratigraphic section of the Spider borehole and displayed in Figure 11. Elements of similar relationship are plotted on Figure 12 and 13 for PC1 vs PC2 and PC 2 vs PC3. For these figures elements with a similar relationship display a positive correlation while elements with opposite relationship display a negative correlation. The inset plot on Figure 12 displays the variation of the lengths of axes of the principal components. In this inset diagram little variation occurs from PC4 onwards, thus only PC1, 2 and 3 are considered to be significant.

PC1 is dominated by a positive co-relationship for Sr, K, Ba, and Rb and negative scores for Fe, Mn, Ni, Ti, and V (Fig. 12).

PC2 is dominated by a positive co-relationship of scores for Fe, Mn, Ti, and V and a negative relationship for As, Cr, and Cu (Fig. 12, 13).

PC3 is dominated by a positive co-relationship of scores for Rb, K, Zn, and As and a negative relationship for Ca (Fig. 13).

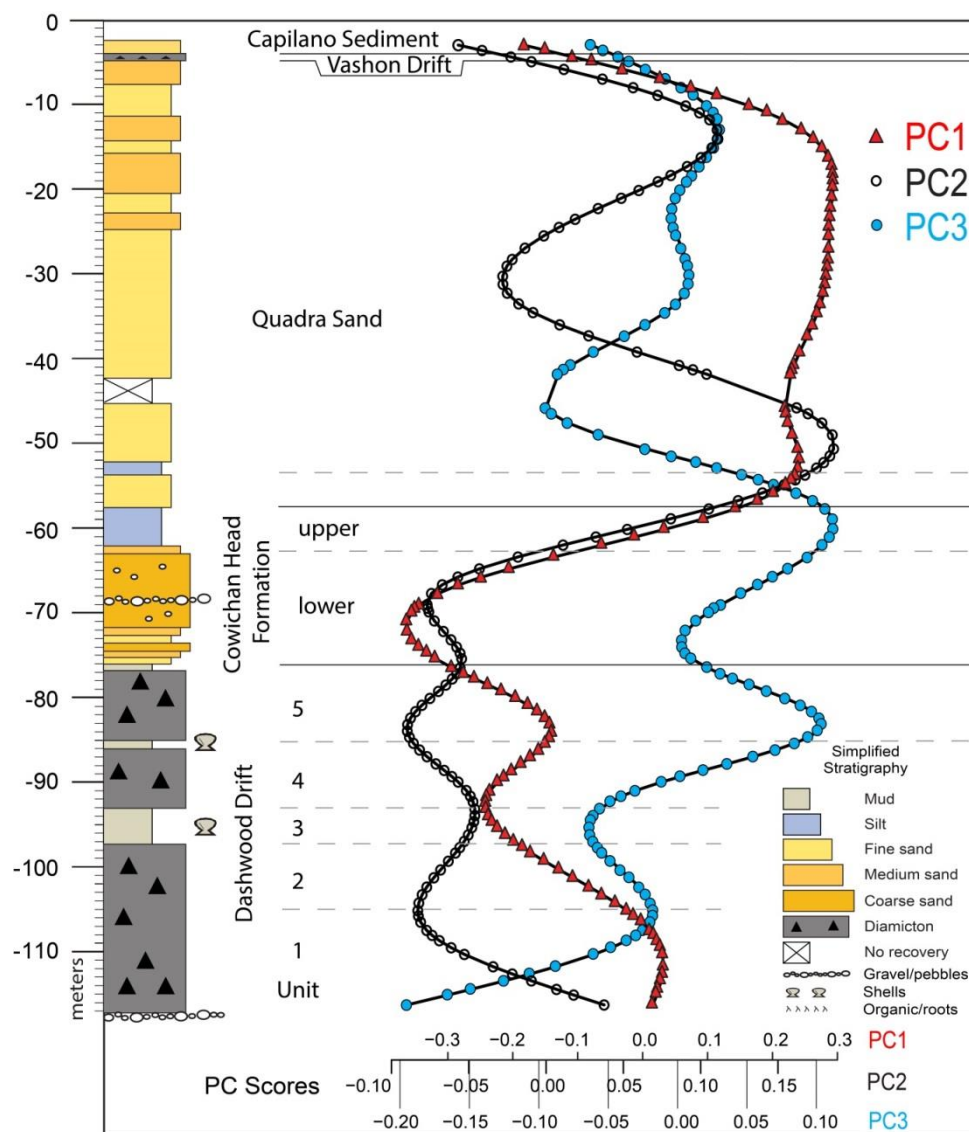


Figure 11. Centered log ratio transformed geochemical data for PC1, PC2 and PC3 plotted adjacent to the Spider borehole stratigraphic section.

#### 4.2.1 Dashwood Drift

For the 41m thick Dashwood Drift 50 analyses were determined from the Spider borehole. These sediments can be subdivided into five units based on changes in sediment character, elemental concentrations and grain size (Appendix B). Some elements such as Cu, Ti (Fig. 14), Cr, Fe, V, and Zn (Appendix B), display an overall increase in concentration or in the case of Sr (Fig. 14) little change in concentration from the base of the formation upwards through the Dashwood Drift and approximately 20 m into the over lying Cowichan Head Formation, even though the silt and clay content decreases at the contact. The lower half of the diamicton sequence displays S concentrations that vary from below detection limit (275 ppm) to a maximum value 720 ppm (AppendixB).

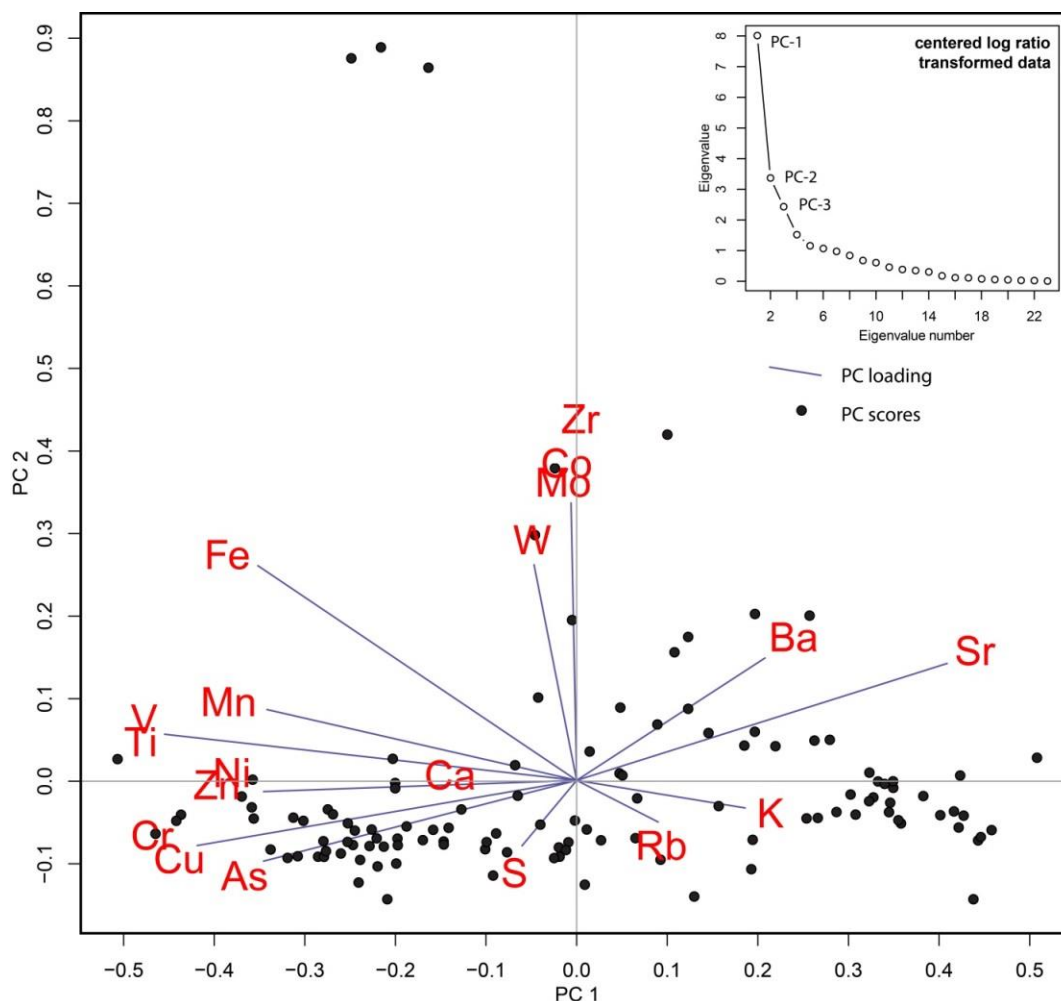


Figure 12. Principal component loading and scores PC1 and PC2 for the Spider data. Elements of similar relationship are plotted as a positive correlation while elements with an opposite relationship plot as a negative correlation. The inset diagram displays the eigenvalues and the number of eigenvectors.

### *Unit 1*

The lower unit comprises a diamicton that is 13 meters thick in core with the basal contact defined by the end of the core. Analyses were determined for 15 samples. The basal portion of this unit consists of a thin horizon of coarse sand and gravel that is reflected with changes in the concentration of Ca, K, Rb, Ti, and V.

### *Unit 2*

The contact between the underlying Unit 1 and Unit 2 occurs at a depth of 104 meters corresponding to an increase in the sand content and a decrease in the clay content. This unit is 7 meters thick. Analyses were determined for 7 samples. Results display a marked decrease in K from a mean of 7899 ppm for unit 1 to mean of 7125 ppm for unit 2, and a slight increase in Ca from a mean of 42899 ppm compared to a mean of 46696 ppm for Unit 2 (Fig. 15). Rb, and Zn also display a decrease in concentrations compared to both the underlying and overlying sediments. The contact between unit 1



and 2 is also defined by a shift in trend for the co-relationship of elements and an inflection point at a depth of 104 meters (dashed line on Fig. 11) that most likely reflects the increased loading of Ca, possibly indicting a change in provenance for sediment between these 2 till units.

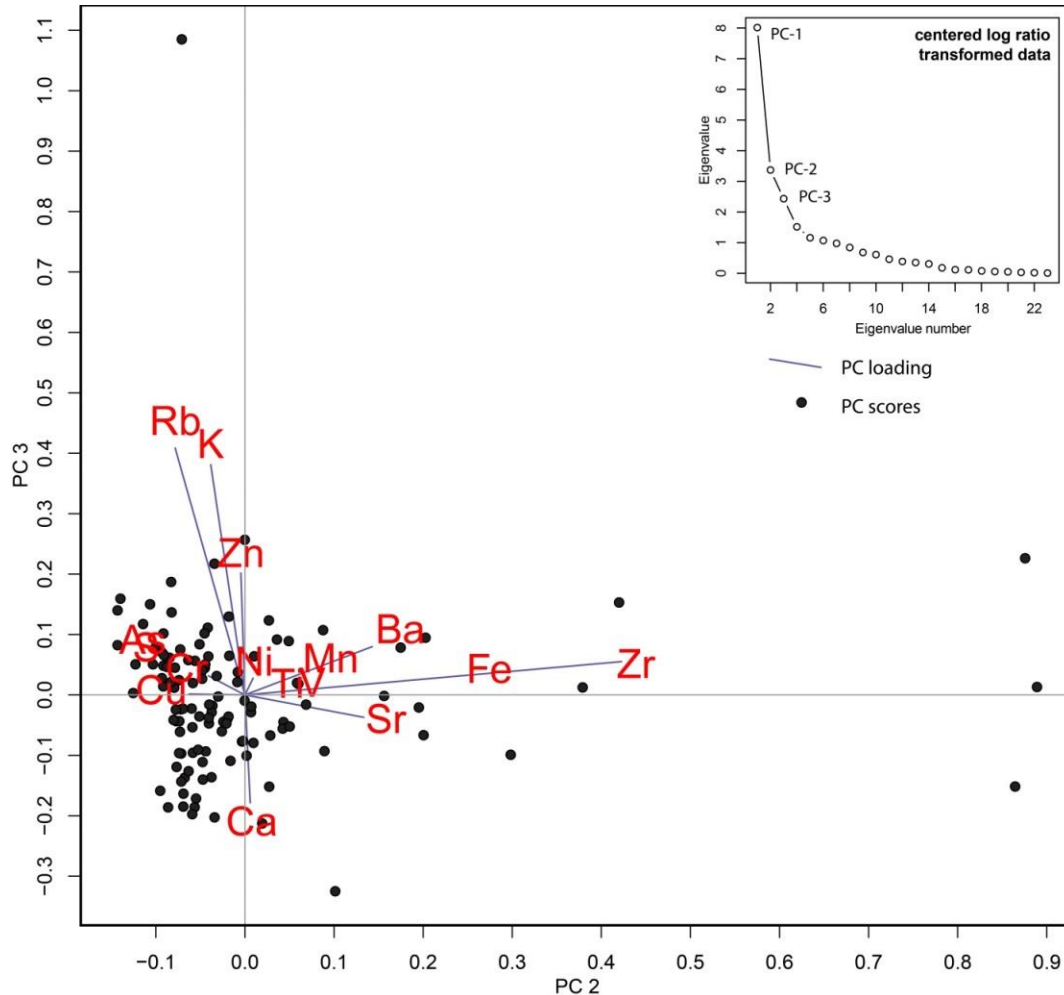


Figure 13. Principal component loading and scores PC2 and PC3 for the Spider data. Elements of similar relationship are plotted as a positive correlation while elements with an opposite relationship plot as a negative correlation. The inset diagram displays the eigenvalues and the number of eigenvectors.

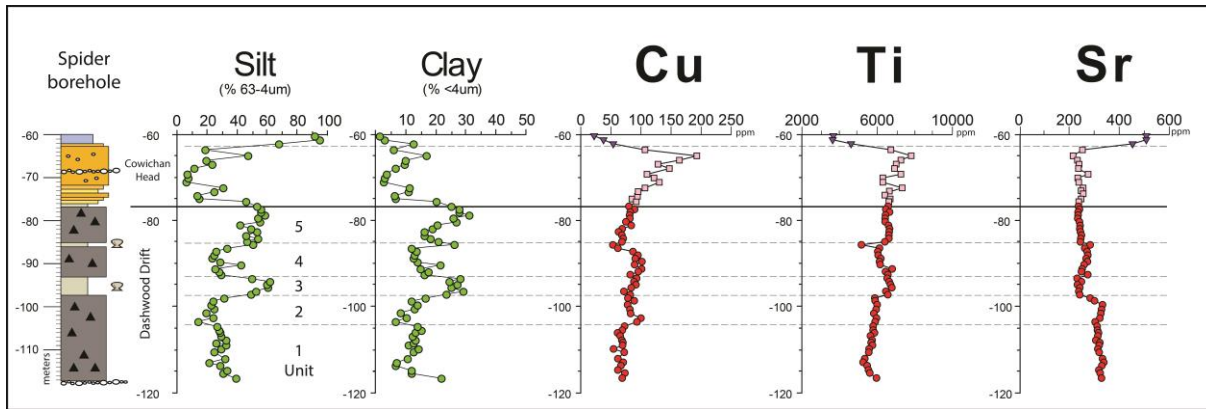


Figure 14. Although there is a decrease in silt and clay content at the Dashwood Drift – Cowichan Head Formation contact some elements including Cu, Ti and Sr continue in concentration trends from the bottom of the Dashwood Drift into the overlying Cowichan Head Formation sediments.

### Unit 3

Six analyses were determined within this 4 m thick mud sequence that contains marine shells. An increase in silt and clay content from 93-97 meters in depth is reflected in an increase in concentration of As, Cr K, (S), Ti and Zn and a decrease in concentration of Ca (Fig. 15) and Sr. Both Ti and Sr display a significant change in concentrations from sediments belonging to units 1 and 2 compared to units 3-5. PC1 and PC2 display a change in the relationship of elements at the contact with the overlying unit 4 sediments (Fig. 11).

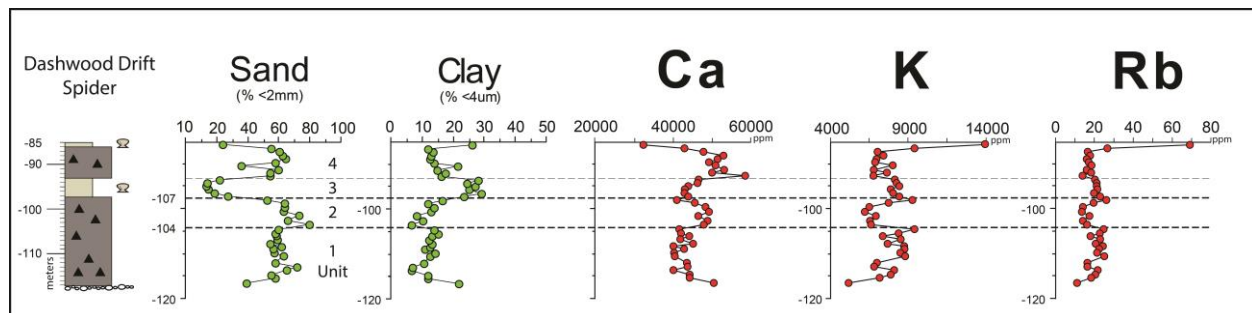


Figure 15. Unit 2 of the Dashwood Drift is defined by an increase in sand content and Ca concentration's and, a decrease in clay content and K and Rb concentrations.

### Unit 4

Unit 4 is composed of a diamicton that is capped by a 1 meter thick mud/clay horizon containing marine shells. Ten analyses were determined from this 7 meter thick unit. The unit displays a marked increase in sand and a corresponding decrease in both silt and clay (Appendix B). Ca and Sr display an increase in concentrations from both the underlying and overlying sediments. The upper 1 meter thick clay horizon displays a spike in concentrations of K, Zn (Fig. 16), Ba, Rb (Appendix B) and a negative spike in Ca, Fe, Mn, Ti, and V (Appendix B). For some elements such as Ba, Ca, there is considerably more variation in concentrations of samples collected from unit 4 compared to those collected from unit 5. The unit 4/5 contact is also visible in the S and Sr concentration changes.

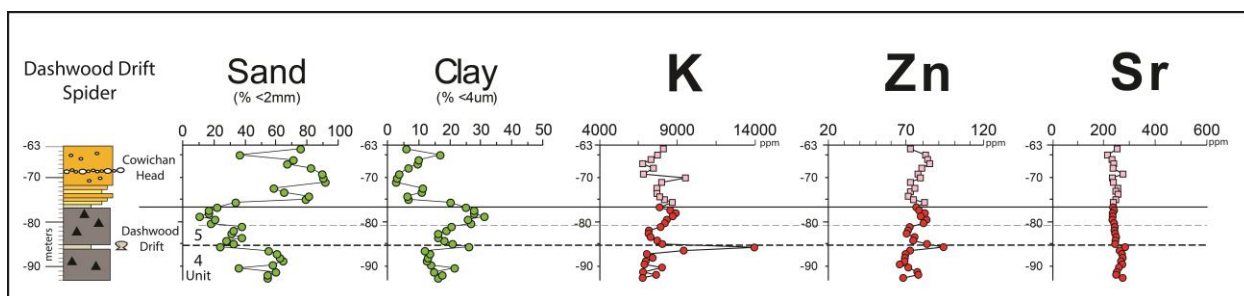


Figure 16. Changes in sand and clay content for unit 5 of the Dashwood Drift are visible in elemental concentration changes for K and Zn while Sr displays no change in concentration.

### Unit 5

Twelve analyses were determined within this 8 meter thick unit. The uppermost sample was collected 5cm below the contact with the overlying Cowichan Head Formation. Unit 5 displays sand contents that are higher in the lower half than the upper half with corresponding changes in silt and clay contents. These changes are visible in both K and Zn concentrations (Fig. 16) but are not detectable for most elements. For example Sr shows no variation through the unit including the 1 meter thick mud/clay at the horizon at the contact with the overlying Cowichan Head Formation Sr is slightly diminished in concentration compared to the underlying unit 4 sediments. The diamicton of unit 5 displays S values with a mean concentration of 688 ppm compared to values mainly below detection limit for both the underlying and overlying sediments.

At a depth of 83 meters PC1, 2, and 3 all display an inflection point (Fig. 11) indicating that there is change in the covariance of multiple element chemistry that is not visible in any single element and is not related to a change in grain size. The contact between the Dashwood Drift and the Cowichan Head Formation is visible with PC2 (Fig. 11). Sediment observations at this contact suggest a sharp boundary, however for elements associated with PC1 and PC3 there is little to no change in the concentration from the Dashwood Drift to the sand of the Cowichan Head Formation suggesting that the sediment provenance does not change.

### 4.2.2 Cowichan Head Formation

Eighteen samples were collected from the 18.5 m thick Cowichan Head for pXRF spectrometry. The formation can be subdivided into a lower oxidized mud rich horizon coarsening-upwards to a coarse-sand. These sediments are overlain by a second coarsening-upwards sequence grading from fine sand to coarse sand with cobbles and gravel lenses. These coarse sands and gravels fine upwards to a medium-sand that is capped by a 4.5 meter thick clay unit similar to the clay horizon at the top of the Cowichan Head Formation in the Cochrane borehole. For the lower Cowichan Head Formation both the sand and silt content vary considerably, however, both an overall lower coarsening-upwards sequence followed by a fining-upwards sequence is depicted in figure 17. The upper Cowichan Head Formation consists of a silt-rich horizon (near 95%) and low sand content.

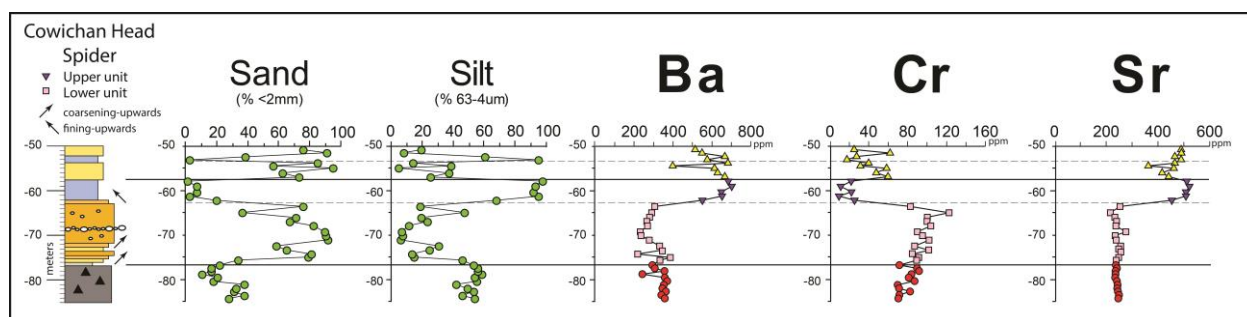


Figure 17. Cowichan Head Formation coarsening-and fining-upwards sequences. For the lower Cowichan Head Formation Ba, Cr, and Sr display geochemical concentrations similar to the underlying Dashwood Drift with upper Cowichan Head Formation elemental concentrations similar to the overlying Quadra Sand.

For most elements the lower and middle portion of the Cowichan Head Formation returns concentrations that are similar to that of the underlying Dashwood Drift. This includes a continual upward increase in concentration for Cr, Cu, Fe, (K), Mn, Ti, V, and Zn (Appendix B). Elements such as Ba and Sr display little to no change in concentration through the upper Dashwood Drift and lower Cowichan Head Formation (Fig. 17). PC3 displays a shift in trend from negative values to positive values at a depth of 74.5 meters corresponding to the top of the coarse-grained sand portion of a coarsening-upwards sequence (Fig 11). At a depth of 72 meters PC1 has a shift in trend from more negative values to positive values at the base of the coarse sand unit while PC2 with a similar trend defines the gravel horizon (-68.5 m) within the coarse sand unit (Fig. 11).

Elemental concentrations of the upper silt display similar values to the overlying Quadra Sand (e.g. Ba, Cr, Cu, Rb, Sr) compared to the underlying lower Cowichan Head Formation coarse sands (Fig. 17). For some elements (Fe, K, Ti) the upper silt unit is very distinct from both the underlying coarse sands and the overlying Quadra Sand (Appendix B).

Overall PC1 displays a significant positive shift towards the base of the Quadra Sand where there are higher concentrations of Sr (Fig. 11).

#### 4.2.3 Quadra Sand

For the 52.5 m thick Quadra Sand 47 analyses were determined. Grain size displays very little variation within the unit (Fig. 18). For some elements the sand displays a distinct geochemical signature compared to the underlying and overlying sediments for Cr, K, Mn, Rb, Ti, and V (Appendix B). For Cu, K and Sr (Fig. 18) and Ba, Ca, and Zn (Appendix B) concentrations are similar to the underlying Cowichan Head Formation. These trends in elemental concentrations correlate with a decrease in silt and clay content. This is especially notable at 54 m depth where there is a contact between medium to fine sand and an overlying 2 meter thick silt horizon. At this contact there is a marked decrease in Ba, Ca, Mn and Sr with an increase in K and a spike in S, the only sample to return a value above detection limits (Appendix B). PC1 displays little variation throughout the Quadra Sand. From 45 m depth to the base of the Quadra Sand PC2 and PC3 display opposite relationships (Fig. 11). This is also somewhat true for a depth of 20 m to 40 m however at the top of the Quadra Sand and both PC2 and PC3 display a similar trend. The strong change in co-relation of elements associated with PC2 and PC3 at a depth of

30 meters suggests that the lower portion of the Quadra Sand represents sediment of a different lithology, provenance and depositional environment however individual element concentrations do not display any significant change in concentration levels. Clague (1976) classifies the depositional environment of the Quadra Sand as a short transport braided river system. Trettin (2004) divides the sands into 2 members, the lower being associated with a high energy, nearshore delta and the upper associated with a fluvial braidplain environment. PC2 and PC3 confirm that there is a difference between the lower and upper portion of the Quadra Sand.

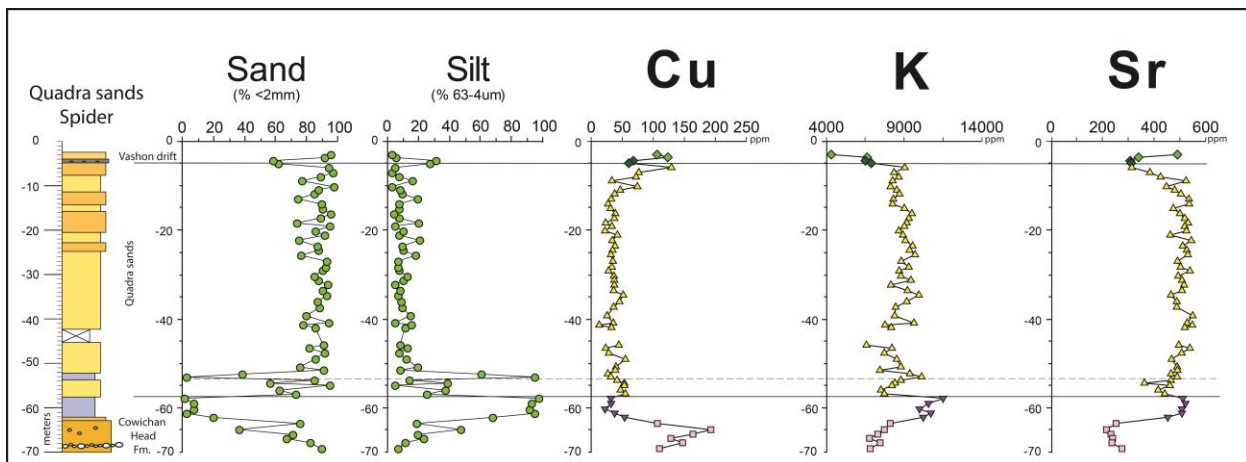


Figure 18. Sand and silt content for the Quadra Sand. Concentrations of Cu and Sr are similar to the underlying upper Cowichan Head Formation whereas K displays concentration's similar to the lower Cowichan Head Formation.

#### 4.2.4 Vashon Drift

For the 1 m thick Vashon drift two analyses were determined. For Cu (Fig. 18), Fe, Mn, and V (Appendix B), there is a marked decrease in the concentration compared to the underlying Quadra Sand and an increase in concentrations with the overlying Capilano Sediments. For Ba, Ca and to a lesser degree K (Fig. 18) there is a marked decrease in concentrations between the Vashon and the overlying Capilano Sediments (Appendix B). PC1, 2, and 3 each display a trend towards negative scores for both the Vashon and Capilano Sediments that may reflect near surface weathering reactions and solubility of some elements.

#### 4.2.5 Capilano Sediments

For 1.5 m thick Capilano Sediments two analyses were determined. With only 2 analyses it is difficult to ascertain geochemical trends in the unit however, there is a decrease in concentration from the underlying Vashon Drift to the Capilano Sediments for Ba, Ca, and Ti. Similarly there is an increase in the concentration for Cu, Fe, Mn, Sr, and V (Fig. 18). These relationships are reflected in the change in grain size between sand, silt and clay content.



## 5.0 Summary

Chemostratigraphic data obtained from the use of a portable X-ray fluorescent spectrometer for samples obtained from a 130 m deep (Cochrane) and the 117 m deep (Spider) borehole can be used to differentiate the sediments based on changes in elemental concentrations. These data can be plotted and compared with the visual stratigraphic sediment descriptions and laboratory grain size analyses. Individual element concentrations can be subjected to multi-element principal component analyses to reduce the number of variables being examined.

From data analyses the lowermost Dashwood Drift displays local variability with probable discontinuous gravel lenses in the lower portion and variable thickness marine clays in the upper portion. Core logging of the till indicates consistency for much of the till; however, changes in both single elemental abundances and multi-element co-relations indicate local variability within these sediments.

For both the Cochrane and Spider boreholes the Cowichan Head Formation sediments directly overlying the Dashwood Drift comprise a few meter thick coarsening-upwards sequence. In the Spider borehole lower Cowichan Head Formation sediments consist of an additional 10 meter thick coarsening-upwards sequence that is not present in the Cochrane borehole. These sands can be differentiated from the overlying upper Cowichan Head Formation sediments and the Quadra Sand by the change in concentration of Cr, Cu, Mn, and Sr (Fig. 19). Hicock and Armstrong (1983) describe two distinct patterns of sedimentation that represent a regional glacial and meltwater system transporting sediments from valleys in the Coast Mountains and more localized fluvial system depositing sediments source from nearby mountain valleys. Data collected here indicates that the source sand/silt/clay of the Dashwood Drift and the lower Cowichan Head Formation are similar in elemental concentration trends, while the upper Cowichan Head Formation and the overlying Quadra Sand display a different trend suggesting that the source for these sediments changed.

For the Quadra Sand the most distinguishing feature is the consistency of Sr concentrations throughout the unit (including the upper Cowichan Head Formation) although there is a decrease in Sr concentrations in the top few meters of the Quadra Sand in the Spider borehole. Sr concentrations are slightly higher in the upper Cowichan Head Formation of the Spider borehole compared to the Quadra Sand. Fe and Ti concentrations are lower than expected given that Crow et al., (2014) report elevated and highly varying magnetic susceptibility values indicating a moderate to significant magnetic mineral content. As suggested by Trettin (2004) and observed here through principal component analyses there is a difference in multiple elemental associations and abundances between the lower and upper Quadra Sand.

The Vashon Drift and Capilano Sediments can be differentiated from each other, and the underlying Quadra Sand, by variations in the concentration of elements such as Ba, Fe, and Mn.

To our knowledge these results are the first systematic geochemical characterization of late Pleistocene succession in the Nanaimo Lowlands. The Cochrane and Spider borehole data demonstrates that pXRF geochemistry is valuable in differentiating stratigraphic units and can provide insight into the provenance of these sediments.

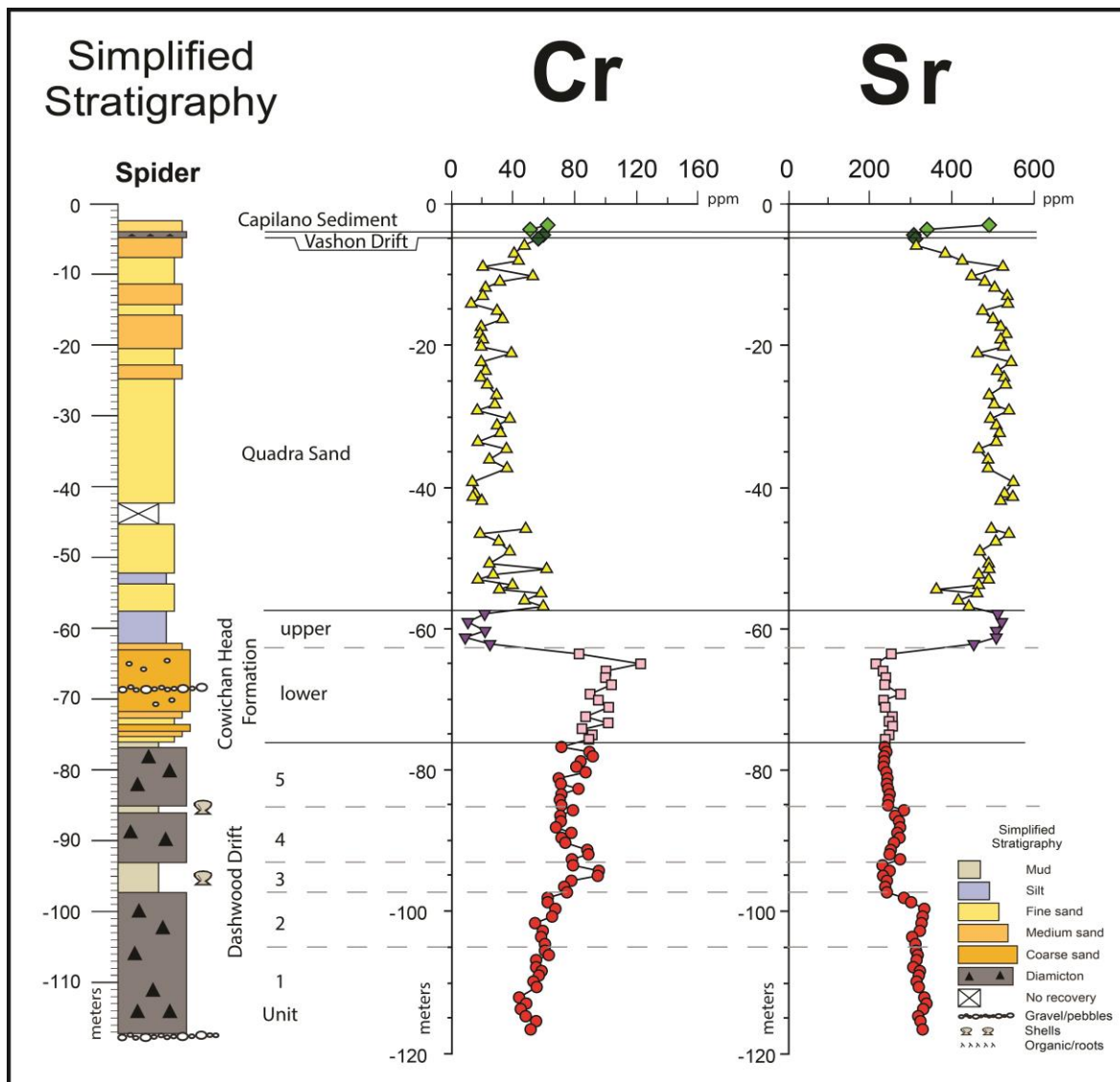


Figure 19. For the Spider borehole Cr and Sr concentrations for the Dashwood Drift and Lower Cowichan Formation display similar trends that are markedly different from the Upper Cowichan Formation and Quadra Sand.

## 6.0 Acknowledgments

Special thanks to Barbara Medioli who helped with the graphical core, sample depth calculations and for her review of the text along with Jan Bednarski. Thanks to Don Cummings for logging the core. Support from drill site geologists Daniel Paradis and Jan Bednarski is much appreciated. This data was collected as part of the Nanaimo Lowlands Aquifer Activity, a collaborative project of the Regional District of Nanaimo and the Aquifer Assessments and Support to Mapping - Groundwater Inventory Project of the Groundwater Geoscience Program, Geological Survey of Canada, Natural Resources Canada.

## 7.0 Referencess

Alley, N.F., 1979. Middle Wisconsin Sstratigraphy and climatic reconstruction, souther Vancouver Island, British Columbia. *Quaternary Research*, v. 11, p. 213-237.

Armstrong, J.E. and Clague, J.J., 1977. Two major Wisconsin lithostratigraphic units in southwestern British Columbia. *Canadian Journal of Earth Sciences*, v. 14, n. 7, p. 1471-1480.

Bednarski, J., 2014. Surficial geology and Pleistocene stratigraphy from Deep Bay to Naoose Harbour, Vancouver Island, British Columbia, Geological Survey of Canada, Open File 7681.

Clague, J.J., 1977. Quadra Sand: a study of Late Pleistocene geology and geomorphic history of coastal southwest British Columbia. Geological Survey of Canada, Paper 77-17, 24 p.

Clague, J.J., 1976. Quadra Sand and its relation to the late Wisconsin glaciation of southwest British Columbia. *Canadian Journal of Earth Sciences*, v. 13, p. 803-815.

Clague, J.J., Froese, D., Hutchinson, I., James, T.S., and Simon, K.M., 2005. Early growth of the last Cordilleran ice sheet deduced from glacio-isostatic depression in southwest British Columbia, Canada. *Quaternary Research*, v. 63, p. 53–59.

Crow, H.L., Knight, R.D., Russell, H.A.J., Pugin, A.J.-M., and Cartwright, T.J., 2014. Downhole geophysical data from five boreholes in the Nanaimo Lowlands, British Columbia; Geological Survey of Canada, Open File 7567, 1 zip file. doi:10.4095/294925.

Crow, H L; Knight, R D; Medioli, B E; Hinton, M J; Plourde, A; Pugin, A J -M; Brewer, K D; Russell, H A J; Sharpe, D R; Geological Survey of Canada, Open File 7079, 2012; 31 pages. doi:10.4095/291486

Dawson, G.M., 1877-1878 . Report of explorations in the southern portion of British Columbia. Report of the Geological Survey of Canada, Part B, p. 105-133.

Fyles, J.G., 1963. Surficial geology of Horne Lake and Parksville map-areas, Vancouver Island, British Columbia. Geological Survey of Canada, Memior 318. 142 p.

Gabrielse, H. and Yorath C.J., 1992. Introduction, Chapter 1 in *Geology of the Cordilleran Orogen in Canada*, Gabrielse, H. and Yorath C.J. (editors), Geological Survey of Canada, n. 4, p. 3-11.

Grunsky, E.C., 2010. The interpretation of geochemical survey data. *Geochemistry: Exploration, Environment, Analysis*, v.10, p. 27-74.

Grunsky, E.C., 2001. A program for computing rq-mode principal components analysis for S-Plus and R. *Computers & Geosciences*, v. 27, p. 229–235.

Hastie, T. J., 1992. Generalized additive models. Chapter 7 of *Statistical Models in S* eds J. M. Chambers and T. J. Hastie, Wadsworth & Brooks/Cole.

Hicock, S.R. and Armstrong, J.E. 1985. Vashon Drift: definition for the formation in the Georgia Depression, southwest British Columbia. *Canadian Journal of Earth Sciences*, v. 22, p. 748-757.

Hicock, S.R. and Armstrong, J.E. 1983. Four Pleistocene formations in southwest British Columbia: their implications for patterns of sedimentation of possible Sangamonian to early Wisconsinan age. *Canadian Journal of Earth Sciences*, v. 20, p. 1232-1247.

Hicock, S.R. and Armstrong, J.E. 1981. Coquitlam Drift: a pre-Vashon Fraser glacial formation in the Fraser Lowland, British Columbia. *Canadian Journal of Earth Sciences*, v. 18, p. 1443-1451.

Knight, R.D., Moroz, M., and Russell, H.J.A. 2012. Geochemistry of a Champlain Sea aquitard, Kinburn, Ontario: portable XRF analysis and fusion chemistry; Geological Survey of Canada, Open File 7085, 1 CD-ROM doi:10.4095/290969

Knight, R.D., Kjarsgaard, B.A., Plourde, A.P., and Moroz, M., 2013. Portable XRF spectrometry of standard reference materials with respect to precision, accuracy, instrument drift, dwell time optimization, and calibration; Geological Survey of Canada, Open File 7358. doi:10.4095/292677

McMartin, I and McClenaghan, M.B., 2001. Till geochemistry and sampling techniques in glaciated shield terrain: a review. In *Drift Exploration in Glaciated Terrains*, ed. by McClenaghan, M.B., Bobrowsky, P.T., Hall, G.E.M., and Cook, S.J. Geological Society of London, Special publication 185, p. 19-43.

Morris, P.A., 2009. Field-portable X-ray fluorescence analysis and its application in QSWA. Geological Survey of Western Australia, Record 2009/7, 23 p.

Mustard, P.S., 1994. The Upper Cretaceous Nanaimo Group, Georgia Basin, in J.W.H. Monger, ed., *Geological Hazards of the Vancouver Region, Southwestern British Columbia*: Geological Survey of Canada, Bulletin 481, p. 27-95.

Plourde, A.P., Knight, R.D., and Russell, H.A.J., 2012. Portable XRF spectrometry of insitu and processed glacial sediment from a borehole within the Spiritwood buried valley, southwest Manitoba; Geological Survey of Canada, Open File 7262. doi:10.4095/291922

Pugin, A. J.-M., Pullan, S. E., and Hunter, J. A., 2009. Multi-component high resolution seismic reflection profiling; *The Leading Edge*, v. 28, p. 1248-1261936-945

Radu, T. and Diamond, D., 2009. Comparison of soil pollution concentrations determined using AAS and portable XRF techniques. *Journal of Hazardous Materials*, v. 171, p. 1168-1171.

Rock, N.M.S., 1988. *Numerical geology*. Springer Verlag, Berlin, p. 427.

Stanley, G., Gallagher, V., NiMhairtin, F., Brogan, J., Lally, P., Doyle, E., and Farrell, L., 2009. Historic mines site inventory and risk classification. *Geochemical characterization and environmental matters*, Geological Survey of Ireland v.1, Appendix 4, p.40.

Thermo Scientific, 2008. Elemental limits of detection in SiO<sub>2</sub> and SRM matrices using soil analysis. Niton XL3t GOLDD + Series x-ray fluorescence analyzer spec sheet.

Trettin, H.P., 2004. Wisconsinan stratigraphy at northern margin of Strait of Georgia, southern Cortes Island and vicinity, British Columbia; Geological Survey of Canada, Current Research 2004-A4, 11 p.

Whitbread, M.A.I., 2004. Lithogeochemical alteration around the Century and elura Zn-Pb-Ag deposits: Detecting alteration expressions in deep and near surface environemnets. PhD. Thesis, University of Canberra, Australia, p.410.

Zhou, D., Chang, T., and Davis, J.C., 1983. Dual extraction of R-mode and Q-mode factor solutions. *Mathematical Geology*, v. 15, p. 581–606.

Zhu, Y., Weindorf, D.C., and Zhang, W., 2011. Characterizing soils using a portable X-ray fluorescence spectrometer: 1. Soil texture. *Geoderma*, v. 167-168, p. 167-177.